

# ASSESSMENT OF PARTICLE MIGRATION EFFECTS IN CAPILLARY RHEOMETRY OF FILLED POLYMERS

*Melquiades Allende and Dilhan M. Kalyon*  
*Department of Chemical, Biochemical and Materials Engineering*  
*Stevens Institute of Technology*  
*Hoboken, NJ 07030*

## Abstract

It is important to assess the conditions under which the migration of particles becomes important during rheological characterization of filled polymers. Such migrations may become important during nonhomogeneous flow where gradients in shear rate induce particles to move away from high shear rate regions resulting in nonhomogeneous concentration distributions and the blunting of velocity distributions. Using the mathematical model of Phillips et al., a finite difference numerical solution was developed to assess the importance of particle migration effects in pressure-driven viscometric flows.

## Introduction

The flow and deformation of filled polymers has been a subject of interest for many years and there has recently been a considerable increase in research activity. The rheological characterization of concentrated suspensions is still a major challenge. Rheological characterization of concentrated suspensions is complicated by microstructural changes that can occur during characterization, including slip at the viscometer walls. Microstructural changes take place during the flow and deformation of even dilute suspensions. For example, Segré and Silberberg [1] have observed that in Poiseuille flow of very dilute suspensions, particles move away from the wall and the center, towards an equilibrium radial position. Wall slip in suspensions is closely related to the formation of an apparent slip layer, which is free of particles. Kalyon and coworkers [2-4] reported that wall slip effects could indeed dominate the apparent rheological behavior of concentrated suspensions.

Shear-induced migration of particles in the transverse direction, even in the absence of inertial effects, has been well documented by Acrivos and coworkers [5-7]. Such migration can alter the concentration distribution, and thus the ultimate properties of extruded articles in the transverse direction and generate complications in rheological characterization. Use of nuclear magnetic resonance (NMR) imaging has provided a substantial amount of experimental evidence to support the claim that unimodal suspensions of rigid spherical particles generate a nonuniform concentration distribution in

nonhomogeneous shear flows [8-11]. In this study, we have extended the model of Phillips et al. [8] by incorporating the apparent wall slip condition at the wall for pressure driven flows. We will focus on the hydrodynamic conditions at which shear-induced particle migration effects are important and when they are insignificant during rheological characterization.

## Background

Phenomenological models for particle migration in shear flows typically attribute migration to irreversible interactions. The first explicit recognition of a cross-stream flux of particles due solely to irreversible interaction effects is due to Leighton and Acrivos [6]. They were motivated by the experimental findings of Gadala-Maria and Acrivos [5]. By using scaling arguments, Leighton and Acrivos [6] were able to derive a general expression for the diffusive flux of particles in simple shear flow. Phillips et al. [8] used a modified version of Leighton and Acrivos [6] flux expression to develop a diffusion equation that describes the evolution of particle concentration over time. This diffusion equation is a phenomenological model that assumes that there are two primary causes for particle migration, particle interactions and local variations of the concentration-dependent suspension viscosity. In our work, the Phillips et al. [8] model was modified by incorporating two boundary conditions that are more realistic, i.e. the continuity of the flux at the axis of symmetry and the incorporation of apparent slip at the wall. Let us first review the Phillips et al. [8] model based on the flux expression of Leighton and Acrivos [6].

Consider a suspension of hard spheres with radius  $a$  in a Newtonian fluid with viscosity  $\eta_s$ . Assume that the particles diffuse in the binder fluid with diffusivity  $D$  and that the Peclet number,  $Pe = a^2 \dot{\gamma} / D$ , is very large so that Brownian motion can be neglected. The particle flux  $\bar{N}_c$ , occurring due to a gradient in collision frequency, is giving by

$$\bar{N}_c = -K_c a^2 \phi \bar{V}(\dot{\gamma} \phi) \quad (1)$$

where  $\dot{\gamma}$  is the magnitude of the local shear rate,  $\phi$  is the particle volume fraction, and  $K_c$  is a proportionality constant of order unity that is found from experimental data. Similarly, the flux  $\bar{N}_\eta$  due to a viscosity gradient, is given by

$$\bar{N}_\eta = -K_\eta a^2 \frac{\dot{\gamma} \phi^2}{\eta} \bar{\nabla} \eta \quad (2)$$

where  $K_\eta$  is a diffusion constant of order unity that is found from experimental data, and  $\eta$  is the shear viscosity of the concentrated suspension. A conservation equation for solid particles can be written in an Eulerian reference frame as

$$\frac{D\phi}{Dt} = -\bar{\nabla} \cdot (\bar{N}_c + \bar{N}_\eta) \quad (3)$$

where  $D/Dt$  is the substantial derivative operator,

$$\frac{D}{Dt} = \frac{\partial}{\partial t} + \bar{\mathbf{v}} \cdot \bar{\nabla} \quad (4)$$

Equation (3) is the shear-induced particle migration equation for a highly concentrated suspension of unimodal spheres undergoing nonhomogeneous shear flows. This equation constitutes the principal result of Phillips et al. [8]. The analysis of flow through a cylindrical tube requires solution of Equation (3) for the case  $\phi = \phi(r, z)$ , where  $r$  is the radial coordinate and  $z$  is the axial coordinate in a cylindrical coordinate system. For this case Equation (3) simplifies to the diffusion equation

$$V_z \frac{\partial \phi}{\partial z} = \frac{a^2}{r} \frac{\partial}{\partial r} \left\{ r \left[ K_c \left( \phi^2 \frac{\partial \dot{\gamma}}{\partial r} + \dot{\gamma} \phi \frac{\partial \phi}{\partial r} \right) + K_\eta \frac{\dot{\gamma} \phi^2}{\eta} \frac{\partial \eta}{\partial r} \right] \right\} \quad (5)$$

Equation (5) is solved with the boundary conditions of the total flux being zero at the solid surface,

$$K_c \left( \phi^2 \frac{\partial \dot{\gamma}}{\partial r} + \dot{\gamma} \phi \frac{\partial \phi}{\partial r} \right) + K_\eta \frac{\dot{\gamma} \phi^2}{\eta} \frac{\partial \eta}{\partial r} = 0 \quad (6)$$

and the symmetry condition at the axis of symmetry,

$$\frac{\partial \phi}{\partial r} = 0. \quad (7)$$

For a given particle distribution  $\phi = \phi(\bar{\mathbf{r}})$ , the velocity and pressure fields are found by solving the equations of motion and continuity,

$$\bar{\nabla} \cdot \bar{\boldsymbol{\tau}} + \bar{\nabla} p = 0 \quad (8)$$

$$\bar{\nabla} \cdot \bar{\mathbf{v}} = 0 \quad (9)$$

with slip velocity boundary condition at the wall,  $u_s$  giving by,

$$u_s = \beta \tau_w \quad (10)$$

where  $\beta$  is the Navier's slip coefficient and  $\tau_w$  is the wall shear stress. The equations of motion and continuity are solved in conjunction with the Newtonian constitutive equation,

$$\bar{\boldsymbol{\tau}} = -\eta(\phi) \underline{\underline{\dot{\gamma}}} \quad (11)$$

where  $\underline{\underline{\dot{\gamma}}} \equiv \bar{\nabla} \bar{\mathbf{v}} + \bar{\nabla} \bar{\mathbf{v}}^t$  is the deformation rate tensor and  $\eta(\phi)$  is the shear viscosity of the concentrated suspension at  $Pe \gg 1$  which is approximated by the Krieger [12] viscosity functional

$$\eta_r = \left( 1 - \frac{\phi}{\phi_m} \right)^{-1.82} \quad (12)$$

where  $\eta_r = \eta(\phi)/\eta_s$  is the relative viscosity of the suspension,  $\eta_s$  is the viscosity of the suspending Newtonian fluid, and  $\phi_m$  is the maximum packing fraction, which is taken as 0.68 for unimodal spheres.

For Poiseuille flow, the  $z$ -component of the equation of motion is solved to give an expression for  $\dot{\gamma}$  as a function of the concentration-dependent suspension viscosity,  $\eta(\phi)$ . Then, Equation (5) is solved to give the particle distribution  $\phi = \phi(r, z)$ . Solution of this initial-value problem also requires specification of the initial distribution  $\phi_0 = \phi(r, 0)$ . We have solved the initial-value problem by the Crank-Nicolson method with a conservative finite-difference scheme in the radial coordinate. In this calculation, values of  $\phi$  at the wall, and of the driving pressure gradient,  $dp/dz$ , are found iteratively until the boundary conditions and volumetric flow rate are satisfied. From experimental data obtained from Couette flow Phillips et al. [8] found that  $K_c/K_\eta = 0.66$  and this ratio was assumed to hold.

## Results and Discussion

Figure 1 shows a set of experimentally obtained particle concentration distribution data [10] for a suspension with  $\phi=0.45$ . This figure also contains the corresponding shear-induced migration model predictions for  $a/R=0.0256$  with the no-slip boundary condition at the wall. It is seen from Figure 1 that the

experimental  $\phi$  profile and the theoretical predictions are qualitatively and quantitatively similar, except at the wall. The disagreement between the experimental  $\phi$  profile and the shear-induced migration model at the wall is related to the constraint on the movement of the particles imposed by the wall and the apparent wall slip. Figure 1 also shows that the theoretical concentration profiles for  $L/D=100$ , 1378 and steady state are indistinguishable. The experimentally determined fully developed velocity profile for the same suspension with  $a/R=0.0256$ , normalized by the average axial velocity, is shown in Figure 2. This figure also contains the corresponding theoretical velocity profiles with the no-slip boundary condition at the wall. As seen in Figure 2 the theoretical velocity profiles agree well with the experimental data except at the wall where the experimental data exhibit a finite slip velocity. Figure 2 also shows that the theoretical velocity profiles for  $L/D=100$ , 1378 and steady state are indistinguishable. The two most prominent features of the experimental data and theoretical predictions for sufficiently large  $a/R$  values are: 1) the nonuniformity of the concentration profiles, which exhibit a maximum value at the axis of symmetry and a minimum value near the tube wall, and 2) the blunting of the velocity profiles.

Figure 3 shows the theoretical predictions for various ratios of particle to capillary radii,  $a/R$ . As seen in Figure 3 the migration rates increase with increasing  $a/R$ . Figure 4 shows that as  $a/R$  increases, the velocity profiles become increasingly blunted, and the maximum velocity decreases. Figure 5 shows the evolution of the wall concentration for different bulk concentrations at a relatively small  $a/R$  ratio of 0.0005. Here  $\langle\phi\rangle$  is the mean bulk (mixing cup) concentration of the particles,  $\langle\phi^w\rangle$  is the mean concentration of the particles at the wall over the entire length of the capillary. The ratio  $(\langle\phi\rangle-\langle\phi^w\rangle)/\langle\phi\rangle$  represents the extent of the deviation of the wall concentration from the bulk concentration during rheological characterization. A negligibly small value of  $(\langle\phi\rangle-\langle\phi^w\rangle)/\langle\phi\rangle$  suggests that particle migration effects are negligible. It is seen from Figure 5 that the change in wall concentration for a small  $a/R$  of 0.0005 is insignificant regardless of the length over diameter ratio of the cylindrical tube. However, as seen in Figure 6, at large  $a/R$ , the wall concentration differs significantly from the bulk concentration. Overall, these results indicate the upper limits in particle migration. This is because the wall slip effect that should reduce the driving force for particle migration has not been considered so far. Let us now see the effect of wall slip. The theoretical velocity profiles for a 50% concentrated suspension, normalized by the average axial velocity, are presented in Figure 7 with a typical slip boundary condition at the wall. The

$(\langle\phi\rangle-\langle\phi^w\rangle)/\langle\phi\rangle$  data in Figure 8 show that the particle migration rate indeed decreases in the presence of wall slip, which decreases the driving force for particle migration.

## Conclusions

Shear-induced particle migration effects become important for relatively large ratio of particle to tube radii,  $a/R$ . The occurrence of wall slip reduces the migration rate of particles. The results presented here can be used to determine the estimates of the upper limits of geometry, flow and suspension characteristics for which particle migration effects need to be considered during rheological characterization of concentrated suspensions.

## Acknowledgments

The helpful comments of Professors E. Cesmebasi, A. Lawal, and C. Tsenoglou are gratefully acknowledged.

## References

1. Segré, G. and A. Silberberg, *Nature, Lond.* **189**, 209 (1961).
2. Yilmazer, U. and D. M. Kalyon, *J. Rheol.* **33**, 1197 (1989).
3. Kalyon, D. M., P. Yaras, B. Aral, and U. Yilmazer, *J. Rheol.* **37**, 35 (1993).
4. Aral, B. and D. M. Kalyon, *J. Rheol.* **38**, 957 (1994).
5. Gadala-Maria, F. and A. Acrivos, *J. Rheol.* **24**, 799 (1980).
6. Leighton, D. and A. Acrivos, *J. Fluid Mech.* **181**, 415 (1987).
7. Jana, S. C., B. Kapoor, and A. Acrivos, *J. Rheol.* **39**, 1123 (1995).
8. Phillips, R. J., R. C. Armstrong, R. A. Brown, A. Graham, and J. R. Abbott, *Phys. Fluids* **A4**, 30 (1992).
9. Altobelli, S. A. and E. Fukushima, *J. Rheol.* **41**, 1105 (1997).
10. Hampton, R. E., A. A. Mammoli, A. L. Graham, N. Tetlow, and S. A. Altobelli, *J. Rheol.* **41**, 621 (1997).
11. Tetlow, N., A. L. Graham, M. S. Ingber, S. R. Subia, L. A. Mondy, and S. A. Altobelli, *J. Rheol.* **42**, 307 (1998).
12. Krieger, I. M., *Adv. Colloid Interface Sci.* **3**, 111 (1972).

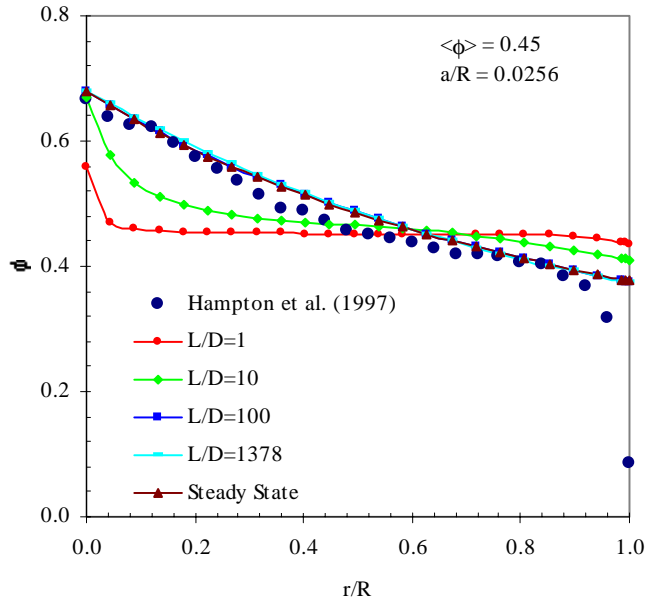


Figure 1. Fully developed experimental particle concentration profile in comparison with model predictions.

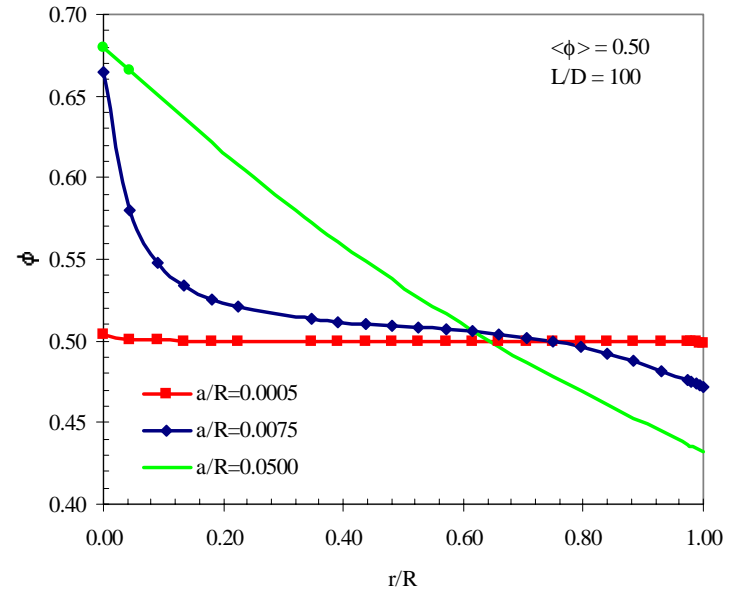


Figure 3. Particle concentration profiles for a 50% concentrated suspension at various  $a/R$  ratios.

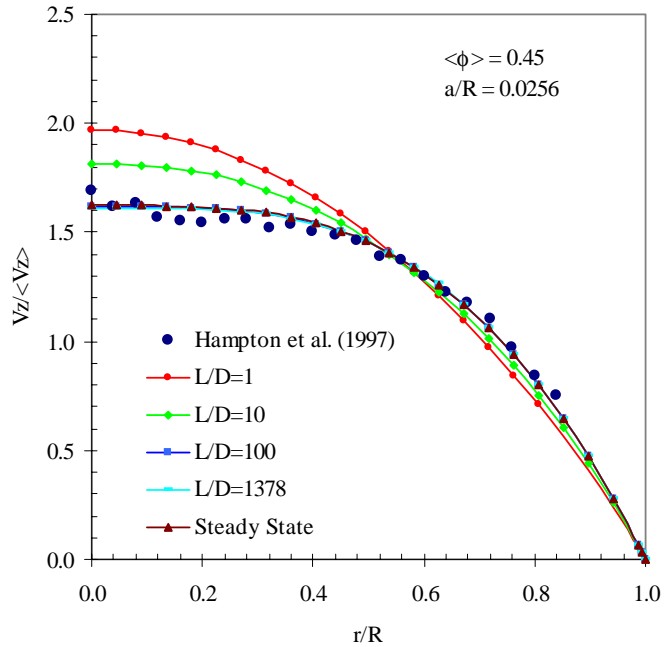


Figure 2. Fully developed experimental normalized velocity profile in comparison with model predictions.

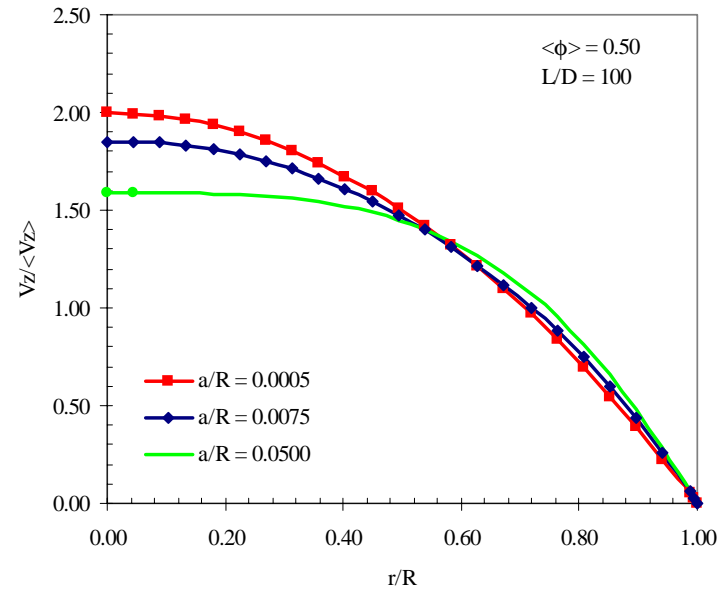


Figure 4. Normalized velocity profiles for a 50% concentrated suspension at various  $a/R$  ratios.

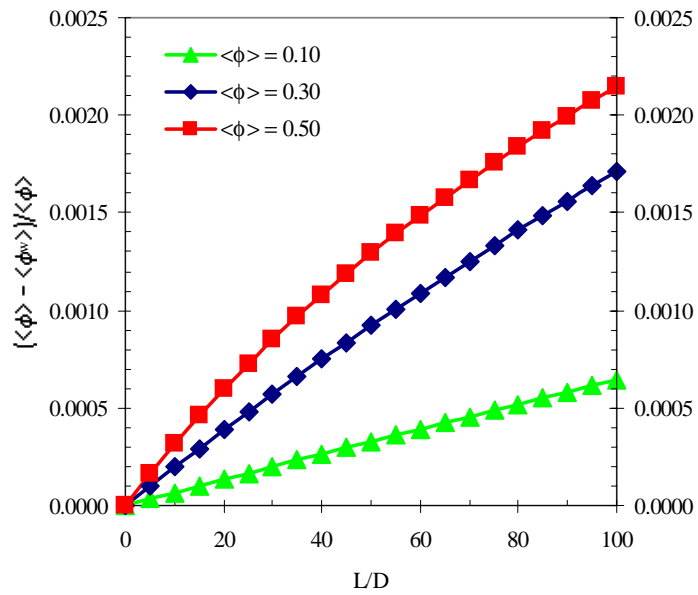


Figure 5. Normalized difference between the bulk concentration,  $\langle\phi\rangle$ , and the axial average wall concentration,  $\langle\phi^w\rangle$ , at  $a/R=0.0005$  for various bulk concentrations.

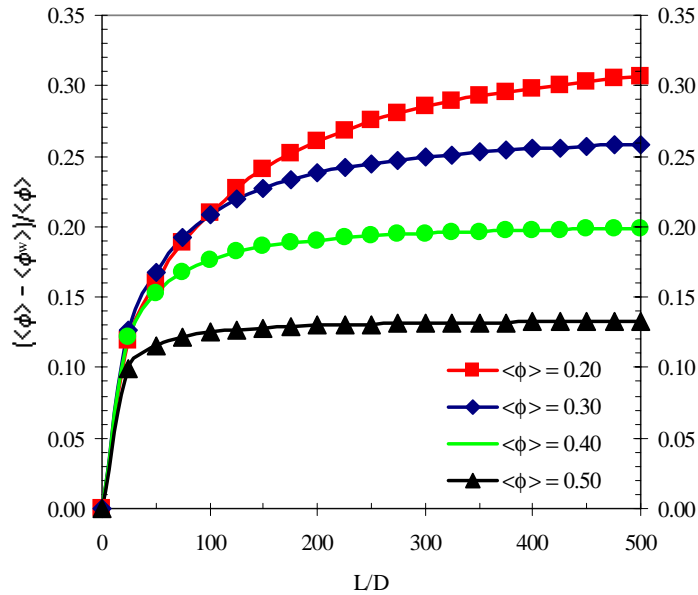


Figure 6. Normalized difference between the bulk concentration,  $\langle\phi\rangle$ , and the axial average wall concentration,  $\langle\phi^w\rangle$ , at  $a/R=0.05$  for various bulk concentrations.

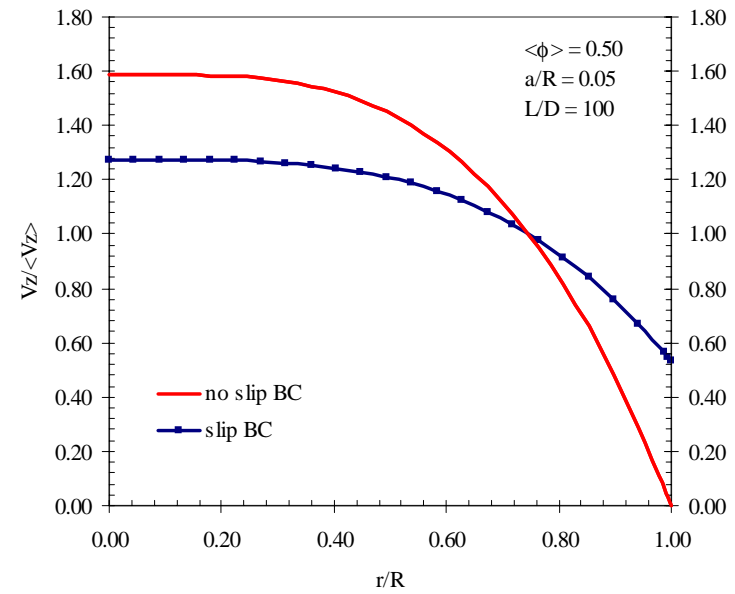


Figure 7. Normalized velocity profiles. The slip coefficient,  $\beta$ , is  $3.5 \times 10^{-5} \text{ m}/(\text{Pa}\cdot\text{s})$ .

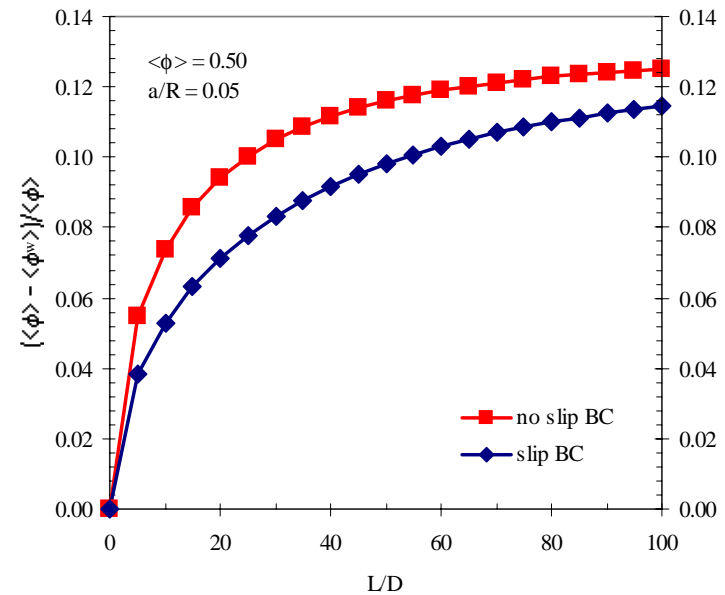


Figure 8. Normalized difference between the bulk concentration,  $\langle\phi\rangle$ , and the axial average wall concentration,  $\langle\phi^w\rangle$ , at  $a/R=0.05$ . The slip coefficient,  $\beta$ , is  $3.5 \times 10^{-5} \text{ m}/(\text{Pa}\cdot\text{s})$ .